JOBS
مجلة العلوم الأساسية
Journal of Basic Science
Print -ISSN 2306-5249
Online-ISSN 2791-3279
العدد السابع والثلاثون
٢٠٢٦م /١٤٤٧هـ
العدد السابع والثلاثون
(607) (585)

تحسين إنتاج البيوسيانين، وهو مستقلب مؤكسد-مختزل، من بكتيريا الزائفة الزنجارية وتقييم فعاليته السامة للخلايا ضد سلالات الخلايا MDA-MB231 و MCF-7

م.د.انفال عز الدين مطر الخطيب
جامعة واسط / كلية التربية الاساسية/ قسم العلوم
anfal@uowasit.edu.iq

المستخلص:

تفرز بكتيريا Pseudomonas aeruginosa صبغة فينازين زرقاء-خضراء تُعرف باسم البيوسيانين(Pyocyanin) ، والتي أصبحت منتجًا طبيعيًا واعدًا لما لها من تأثيرات قوية مضادة للميكروبات ومضادة للسرطان. يركّز هذا البحث على تحسين ظروف إنتاج البيوسيانين من بكتيريا P. aeruginosa ودراسة تأثيره السام على الخلايا السرطانية ضد خطّي خلايا سرطان الثدي البشري MDA-MB231 و MCF-7. ومن خلال تحسين دقيق للعوامل الغذائية والبيئية مثل مصدر الكربون، مصدر النيتروجين، الرقم الهيدروجيني(pH) ، درجة الحرارة، ومدة الحضانة، تم الحصول على أعلى كمية من البيوسيانين. وقد استُخدمت التصاميم الإحصائية للتجارب، بما في ذلك منهجية سطح الاستجابة(Response Surface Methodology) ، لتحديد العوامل الأكثر تأثيرًا في إنتاج الصبغة.

بعد ذلك، تم تنقية البيوسيانين وتجفيفه بالتجميد(Lyophilization) ، ثم تقييم نشاطه المضاد للسرطان باستخدام اختبار MTT والفحص المظهري للخلايا. وأظهرت النتائج أن ظروف الإنتاج المحسّنة أدت إلى إنتاج كمية عالية من البيوسيانين مقارنةً بالأوساط الغذائية الأساسية، وكانت هذه الكمية كافية لاستخدامها كعامل علاجي محتمل. أُجريت اختبارات السمية الخلوية، ولوحظ تثبيط معتمد على الجرعة لتكاثر الخلايا السرطانية في سرطان الثدي، حيث أظهر كلّ من خطّي الخلايا MDA-MB231و MCF-7 حساسية تجاه البيوسيانين. كما تم حساب قيمة IC_{50} ، ودراسة مسارات موت الخلايا مثل الاستماتة (Apoptosis) والنخر (Necrosis) باستخدام الفحص المجهري وقياس التدفق الخلوي (Flow Cytometry). توفّر هذه الدراسة معلومات علمية مهمة

JOBS مجلة العلوم الأساسية Journal of Basic Science
Print -ISSN 2306-5249
Online-ISSN 2791-3279
العدد السابع والثلاثون
٢٠٢٦م /١٤٤٧هـ

حول الإنتاج واسع النطاق للبيوسيانين، وتؤكد إمكانية استخدامه كعامل طبيعي مضاد للسرطان، مما يستدعي إجراء المزيد من الأبحاث السريرية المستقبلية.

الكلمات المفتاحية: البيوسيانين، Pseudomonas aeruginosa، منهجية الاستجابة السطحية، السمية الخلوية، النشاط المضاد للسرطان، MDA-MB231، MCF-7

Optimization of Pyocyanin, a Redox Metabolite, Production from Pseudomonas aeruginosa and Evaluation of its Cytotoxic Efficacy against MDA-MB231 and MCF-7 Cell Lines

Anfal Izaldeen Mutar AL KATEEB
anfal@uowasit.edu.iq
Wasit University/College of Basic Education.
Branch of Biology/Department of Science

Abstract

Pseudomonas aeruginosa secretes a blue-green phenazine pigment known as pyocyanin, a redox metabolite that has emerged as a promising natural compound with potent antimicrobial and anticancer properties. This study was designed to optimize pyocyanin production conditions from clinical isolates of P. aeruginosa and to evaluate its cytotoxic activity against two human breast cancer cell lines, MDA-MB231 and MCF-7. Nutritional and environmental parameters — including carbon source, nitrogen source, pH, temperature, and incubation time — were systematically optimized to maximize pyocyanin yield. Statistical experimental designs based on response surface methodology (RSM) were employed to identify the factors most significantly influencing pigment production. The purified, lyophilized pyocyanin was subsequently assessed for anticancer activity using the MTT assay and morphological examination.

Findings indicated that optimized production conditions yielded significantly higher pyocyanin levels compared to basal media, demonstrating sufficient quantities for potential therapeutic application. Cytotoxicity assays revealed dose-dependent inhibition of breast cancer cell proliferation, with both MDA-MB231 and MCF-7 cell lines demonstrating sensitivity to pyocyanin treatment. IC_{50} values were determined, and cell death pathways, including apoptosis and necrosis, were characterized through fluorescence microscopy

and flow cytometry. In conclusion, optimized conditions significantly enhanced pyocyanin production from Pseudomonas aeruginosa. The purified compound exhibited dose-dependent cytotoxicity against MDA-MB-231 and MCF-7 breast cancer cells, inducing apoptosis and necrosis, suggesting its promising potential as a natural anticancer agent.

Keywords: Pyocyanin, Pseudomonas aeruginosa, optimization, cytotoxicity, breast cancer

1. Introduction

Pseudomonas aeruginosa is a Gram-negative bacterium renowned for its extensive capacity to produce diverse secondary metabolites, among which pyocyanin is considered one of the most significant virulence factors (Al Kateeb et al., 2022). This blue-green phenazine compound has attracted considerable scientific interest not only for its roles in bacterial physiology and pathogenesis but also for its substantial therapeutic potential. Growing concern over the escalating resistance to antimicrobial agents and the limited efficacy of conventional cancer therapies has prompted investigators to explore bioactive natural compounds as alternative therapeutic candidates (Das et al., 2022). Pyocyanin represents a particularly compelling candidate owing to its distinctive redox properties and its capacity to induce oxidative stress selectively in mammalian cells. The compound functions as an electron shuttle that generates reactive oxygen species (ROS) capable of preferentially targeting cancer cells, which typically exhibit diminished antioxidant defenses relative to normal cells (El-Fouly et al., 2015).

The biosynthesis of pyocyanin in P. aeruginosa is tightly regulated by quorum sensing, particularly via the PQS pathway (Tüfekci et al., 2020). The biosynthetic cascade originates from chorismic acid and proceeds through a series of enzymatic reactions encoded by the phz gene cluster, culminating in the formation of phenazine-1-carboxylic acid (PCA). The PhzM and PhzS enzymes subsequently catalyze the conversion of PCA into pyocyanin. Recent advances in elucidating this biosynthetic pathway have facilitated efforts to enhance pyocyanin production through environmental and nutritional optimization, while wild-type strains remain indispensable for medical applications due to regulatory requirements. The primary objective

of production optimization is to maximize yield without compromising the compound's structural integrity and bioactivity (Mabrouk et al., 2014).

The anticancer potential of pyocyanin has been previously investigated across various cancer cell lines, with particular emphasis on breast cancer due to its high global prevalence and the ongoing need for novel therapeutic strategies. Triple-negative breast cancer (TNBC), represented by MDA-MB-231 cells, is among the most aggressive and frequently diagnosed subtypes worldwide. This subtype is characterized by poor prognosis, therapeutic resistance, and lack of responsiveness to conventional hormone-based treatments (M Abdel Rasool et al., 2025). The MCF-7 cell line, representing hormone receptor-positive breast cancer, provides a complementary model for evaluating the efficacy of pyocyanin across distinct breast cancer subtypes (Izaldeen et al., 2024). Pyocyanin has been demonstrated to induce cell death through multiple mechanisms, including oxidative stress induction, mitochondrial dysfunction, and activation of apoptotic pathways. Its capacity to generate ROS renders it particularly effective against metabolically active cancer cells, which exhibit heightened susceptibility to oxidative stress compared to normal cells (Abdelaziz et al., 2022).

Although pyocyanin holds considerable anticancer promise, several challenges must be addressed before translation from bench to bedside. These include optimizing production to yield economically viable quantities, ensuring purity and consistency of the extracted compound, elucidating precise mechanisms of action across diverse cancer types, and establishing appropriate dosage regimens that maximize therapeutic efficacy while minimizing toxicity to normal cells. The present study addresses these challenges by systematically optimizing pyocyanin production and conducting comprehensive cytotoxicity assays on breast cancer cell lines, thereby establishing a scientific foundation for future therapeutic advancement.

2. Materials and Methods

2.1Bacterial Strain and Culture Conditions

Clinical isolates of Pseudomonas aeruginosa were obtained from urine specimens submitted to the clinical microbiology laboratory. Isolates were

JOBS مجلة العلوم الأساسية
Journal of Basic Science
Print -ISSN 2306-5249
Online-ISSN 2791-3279
العدد السابع والثلاثون
٢٠٢٦م /١٤٤٧هـ

stored as glycerol stocks at −80°C for long-term preservation of genetic stability. Initial screening for pyocyanin production was performed by cultivating isolates in King's A medium and visually inspecting for the characteristic blue-green pigmentation. The most productive isolate was selected for subsequent optimization studies. For routine cultivation, isolates were grown in Luria-Bertani (LB) broth at 37°C with continuous agitation at 180 rpm for 48 hours (Abdelaziz et al., 2022).

2.2 Screening of Nutritional Parameters

Preliminary screening experiments were conducted to identify the nutritional and environmental factors most significantly influencing pyocyanin production. Carbon sources evaluated included glucose, glycerol, sucrose, fructose, and mannitol at concentrations ranging from 0.5% to 2% (w/v). Nitrogen sources assessed comprised peptone, yeast extract, beef extract, ammonium sulfate, ammonium chloride, and sodium nitrate, each at 0.5% to 1.5% (w/v). Additional parameters examined included magnesium sulfate concentration, potassium phosphate concentration, pH (5.0–9.0), temperature (28°C–42°C), and incubation time (24–96 hours). Each parameter was assessed individually using a one-factor-at-a-time (OFAT) approach to generate baseline data for subsequent statistical optimization (Bacame-Valenzuela et al., 2020).

2.3Statistical Optimization Using Response Surface Methodology

Variables identified as most influential through preliminary screening were further optimized using response surface methodology (RSM). A Box-Behnken design was employed, incorporating three factors at three levels each: glycerol concentration (1.0–2.0% w/v), pH (6.0–8.0), and temperature (33–37°C). The experimental design comprised 17 runs with five center points to estimate experimental error. The coefficient of determination (R^2) and adjusted R^2 were calculated to evaluate model adequacy (Gahlout et al., 2021).

2.4Pyocyanin Extraction and Purification

Pyocyanin was extracted from cell-free culture supernatants using a modified chloroform extraction protocol. Bacterial cultures were centrifuged at 10,000 rpm at 4°C to remove cellular biomass. Chloroform was added to the supernatant at a 2:1 (v/v) ratio and vigorously mixed for 10 minutes. The organic phase containing pyocyanin was separated and re-extracted with 0.2 N HCl, transferring the pigment into the aqueous phase as a pink-red solution. Alkalinization with 1 N NaOH restored the characteristic blue color, and the compound was re-extracted with chloroform. The final chloroform extract was evaporated under reduced pressure using a rotary evaporator at 45°C to obtain crude pyocyanin crystals. The crude extract was dissolved in minimal chloroform and purified by silica gel column chromatography with chloroform-methanol gradient elution. Fractions were analyzed spectrophotometrically at 520 nm and 690 nm to identify pure pyocyanin-containing fractions (Mavrodi et al., 2001).

2.5 Characterization of Purified Pyocyanin

The purified pyocyanin was characterized using multiple analytical techniques. UV-visible spectroscopy was performed by scanning from 200 to 800 nm to confirm characteristic absorption peaks at 280, 380, 520, and 690 nm. Fourier-transform infrared spectroscopy (FTIR) was employed to identify functional groups, with samples prepared as KBr pellets and scanned from 400 to 4000 cm^{-1}. Purity was assessed by high-performance liquid chromatography (HPLC) using a C18 column with a methanol-water mobile phase and detection at 280 nm. Mass spectrometry was performed to confirm molecular weight and structural identity. Purified pyocyanin was lyophilized and stored at −20°C in amber vials protected from light until use in cytotoxicity assays (Elbargisy, 2021).

2.6 Cell Culture and Maintenance

MDA-MB231 (triple-negative) and MCF-7 (estrogen receptor-positive) human breast adenocarcinoma cell lines were obtained from the American Type Culture Collection (ATCC). Cells were maintained in Dulbecco's Modified Eagle Medium (DMEM) supplemented with 10% fetal bovine serum (FBS), 100 units/mL penicillin, and 100 µg/mL streptomycin under a humidified atmosphere of 5% CO_2 at 37°C. Subculturing was performed

every 3–4 days at 80–90% confluence using 0.25% trypsin-EDTA. Cell viability was routinely assessed by trypan blue exclusion assay, and only cultures exhibiting viability exceeding 95% were used. Cells at passages 5–20 were employed to ensure experimental consistency (Al Kateeb et al., 2022).

2.7 MTT Cytotoxicity Assay

The cytotoxic activity of pyocyanin was assessed using the 3-(4,5-dimethylthiazol-2-yl)-2,5-diphenyltetrazolium bromide (MTT) assay. Cells were seeded at a density of 5×10^3 cells per well in 96-well plates and allowed to adhere overnight. A stock solution was prepared in DMSO and serially diluted in culture medium to achieve final concentrations of 1.56–200 µg/mL, with DMSO maintained below 0.5% (v/v) in all wells. After 24, 48, and 72 hours of treatment, MTT solution was added to a final concentration of 0.5 mg/mL and incubated for 4 hours. Formazan crystals were dissolved in DMSO, and absorbance was measured at 570 nm using a microplate reader. Cell viability was expressed as a percentage relative to untreated controls, and IC_{50} values were calculated by nonlinear regression analysis (Jayaseelan et al., 2014).

2.8 Morphological Analysis

Morphological alterations in pyocyanin-treated cancer cells were evaluated by phase-contrast microscopy. Cells were seeded at 2×10^5 cells per well in 6-well plates and treated with pyocyanin at IC_{25}, IC_{50}, and IC_{75} concentrations. Observations were made at 200× magnification at 24 and 48 hours post-treatment, and photomicrographs were recorded. Apoptotic features, including cell shrinkage, membrane blebbing, nuclear condensation, and apoptotic body formation, were documented. Acridine orange/ethidium bromide (AO/EB) dual staining was performed to distinguish viable, early apoptotic, late apoptotic, and necrotic cells under fluorescence microscopy (Abdelaziz et al., 2022).

2.9 Flow Cytometry Analysis

Apoptosis induction was quantitatively assessed using Annexin V-FITC/propidium iodide (PI) double staining and flow cytometry. Cells were treated with an IC_{50} concentration of pyocyanin for 24 and 48 hours, then

harvested by trypsinization and washed twice with cold phosphate-buffered saline (PBS). Cells were resuspended in binding buffer and stained with Annexin V-FITC and PI according to the manufacturer's protocol. A minimum of 10,000 events per sample were acquired using a flow cytometer, and data were analyzed using FlowJo software. Cells were classified into four populations: viable (Annexin V^-/PI^-), early apoptotic (Annexin V^+/PI^-), late apoptotic (Annexin V^+/PI^+), and necrotic (Annexin V^-/PI^+) (Perużyńska, 2025).

2.10 Statistical Analysis

All experiments were performed in triplicate, and results are expressed as mean ± standard deviation (SD). One-way analysis of variance (ANOVA) with Tukey's post-hoc test was used for multiple group comparisons, and Student's t-test was applied for pairwise comparisons. P-values less than 0.05 were considered statistically significant. IC_{50} values were calculated using nonlinear regression curve fitting in GraphPad Prism. Response surface methodology data were analyzed using Design-Expert software to generate predictive models and optimize production parameters (Abo-Zaid et al., 2015).

3. Results and Discussion

3.1 Screening of Production Parameters

Preliminary screening experiments demonstrated that both carbon and nitrogen sources exerted significant effects on pyocyanin production. Among the carbon sources evaluated, glycerol yielded the highest pyocyanin concentration (48.3 µg/mL), surpassing glucose (35.7 µg/mL) and sucrose (28.4 µg/mL). The superior performance of glycerol is consistent with its dual role as a carbon source and redox regulator, which may facilitate upregulation of phenazine-biosynthetic gene expression. With respect to nitrogen sources, peptone yielded the greatest pyocyanin output (52.1 µg/mL), significantly outperforming yeast extract (41.8 µg/mL) and ammonium sulfate (29.3 µg/mL). The superiority of organic nitrogen sources likely reflects their capacity to supply essential amino acids and peptides that

JOBS
مجلة العلوم الأساسية
Journal of Basic Science
Print -ISSN 2306-5249
Online-ISSN 2791-3279
العدد السابع والثلاثون
٢٠٢٦م /١٤٤٧هـ

support bacterial growth and secondary metabolite biosynthesis more effectively than inorganic nitrogen forms (Abdelaziz et al., 2022).

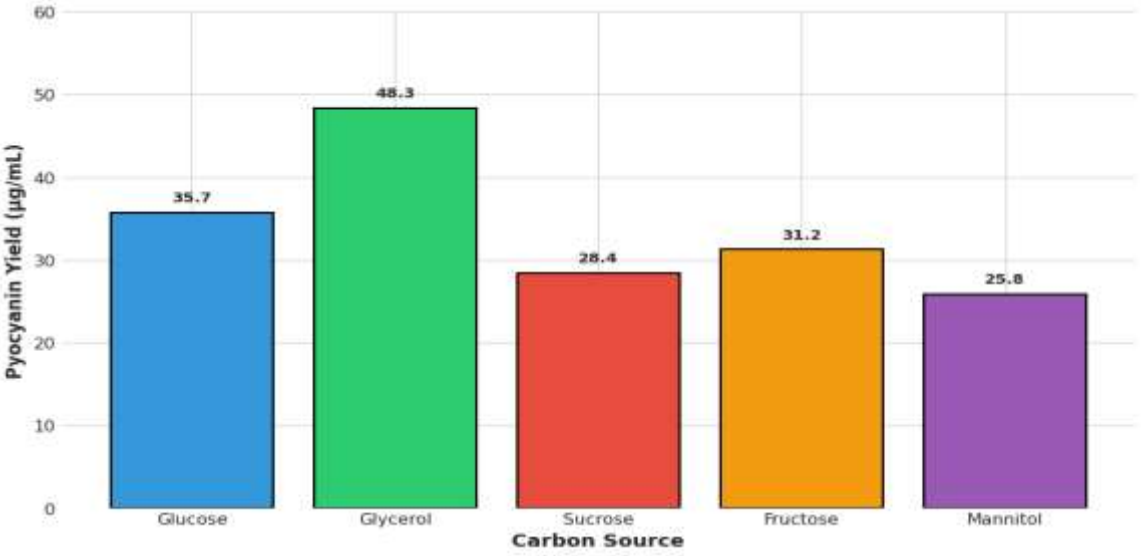

Figure 1: Effect of carbon sources on pyocyanin yield following 48 hours of incubation.

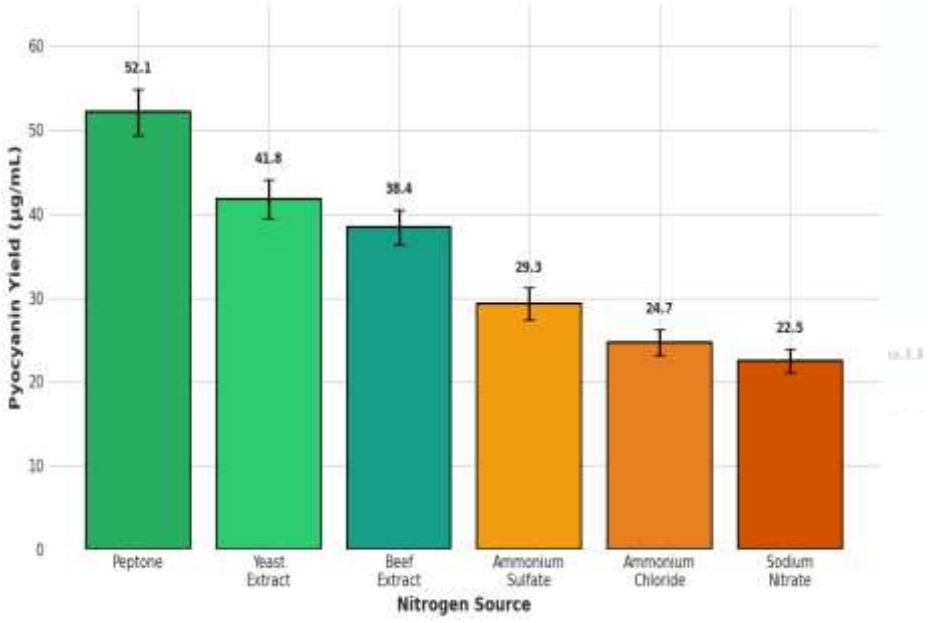

Figure ٢: Relative pyocyanin production with various nitrogen sources.

pH optimization revealed that P. aeruginosa achieves maximal pyocyanin production under neutral to slightly alkaline conditions, with a peak yield of

JOBS مجلة العلوم الأساسية Journal of Basic Science
Print -ISSN 2306-5249
Online-ISSN 2791-3279
العدد السابع والثلاثون
٢٠٢٦م /١٤٤٧هـ

58.6 µg/mL at pH 7.0 and markedly reduced yields of 22.5–38.4 µg/mL at acidic pH values (5.0–6.0). Alkaline conditions exceeding pH 8.0 similarly attenuated production, indicating that quorum-sensing-mediated phenazine biosynthetic gene expression is optimally sustained within a narrow pH range. Temperature optimization identified 35°C as the optimal growth temperature, yielding 61.2 µg/mL, with substantially reduced production below 30°C and above 39°C, consistent with the physiological preferences of P. aeruginosa and temperature-dependent virulence factor regulation. Time-course analysis demonstrated that maximal pyocyanin accumulation occurred between 48 and 60 hours of incubation, with subsequent decline attributable to nutrient depletion and metabolic shifts associated with the stationary phase (Bacame-Valenzuela et al., 2020).

3.2 Response Surface Methodology Optimization

The Box-Behnken design facilitated systematic investigation of variable interactions to determine conditions maximizing pyocyanin production. Analysis of variance of the quadratic model revealed high statistical significance ($p < 0.0001$), with an F-value of 127.43 confirming that the model effectively described the experimental data. The coefficient of determination ($R^2 = 0.9876$) and adjusted R^2 (0.9717) confirmed excellent model fit and predictive capacity. The non-significant lack of fit ($p = 0.128$) further validated model adequacy. A regression equation was derived to predict pyocyanin yield as a function of the three independent variables and their interactions (Gahlout et al., 2021).

Table 1: Box-Behnken experimental design matrix and pyocyanin production.

Run	Glycerol (% w/v)	pH	Temperature (°C)	Pyocyanin Yield (µg/mL)
1	1.0	6.0	35	42.5 ± 2.1
2	2.0	6.0	35	51.3 ± 2.8
3	1.0	8.0	35	38.7 ± 1.9
4	2.0	8.0	35	47.2 ± 2.4
5	1.0	7.0	33	45.8 ± 2.2
6	2.0	7.0	33	58.6 ± 3.1

JOBS
مجلة العلوم الأساسية
Journal of Basic Science
Print -ISSN 2306-5249
Online-ISSN 2791-3279
العدد السابع والثلاثون
٢٠٢٦م /١٤٤٧هـ

7	1.0	7.0	37	40.3 ± 2.0
8	2.0	7.0	37	53.9 ± 2.7
9	1.5	6.0	33	48.2 ± 2.3
10	1.5	8.0	33	44.5 ± 2.2
11	1.5	6.0	37	45.1 ± 2.3
12	1.5	8.0	37	41.8 ± 2.1
13	1.5	7.0	35	62.4 ± 3.2
14	1.5	7.0	35	61.8 ± 3.1
15	1.5	7.0	35	63.1 ± 3.3
16	1.5	7.0	35	62.0 ± 3.0
17	1.5	7.0	35	62.7 ± 3.2

Table 2: ANOVA outputs of the quadratic model for pyocyanin production.

Source	Sum of Squares	df	Mean Square	F-value	P-value
Model	1456.32	9	161.81	127.43	< 0.0001
Glycerol	385.47	1	385.47	303.52	< 0.0001
pH	142.28	1	142.28	112.02	< 0.0001
Temperature	89.63	1	89.63	70.58	< 0.0001
Glycerol × pH	28.45	1	28.45	22.40	0.0018
Glycerol × Temp	15.82	1	15.82	12.46	0.0091
pH × Temp	8.73	1	8.73	6.87	0.0334
Glycerol²	98.34	1	98.34	77.43	< 0.0001
pH²	156.72	1	156.72	123.41	< 0.0001
Temperature²	74.18	1	74.18	58.41	< 0.0001
Residual	8.89	7	1.27	—	—
Lack of Fit	4.23	3	1.41	1.21	0.128
Pure Error	4.66	4	1.17	—	—
Total	1465.21	16	—	—	—

R^2 = 0.9876; Adjusted R^2 = 0.9717; Predicted R^2 = 0.9512

JOBS
مجلة العلوم الأساسية
Journal of Basic Science
Print -ISSN 2306-5249
Online-ISSN 2791-3279
العدد السابع والثلاثون
٢٠٢٦م /١٤٤٧هـ

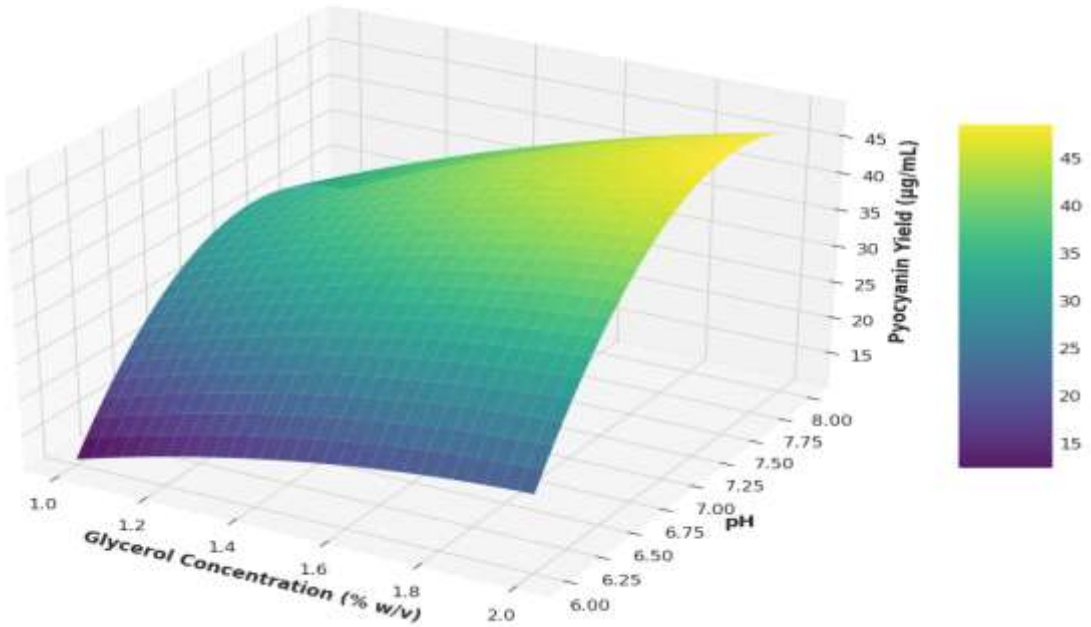

Figure ٣: 3D response surface plot illustrating the interaction between glycerol concentration and pH on pyocyanin production at 35°C.

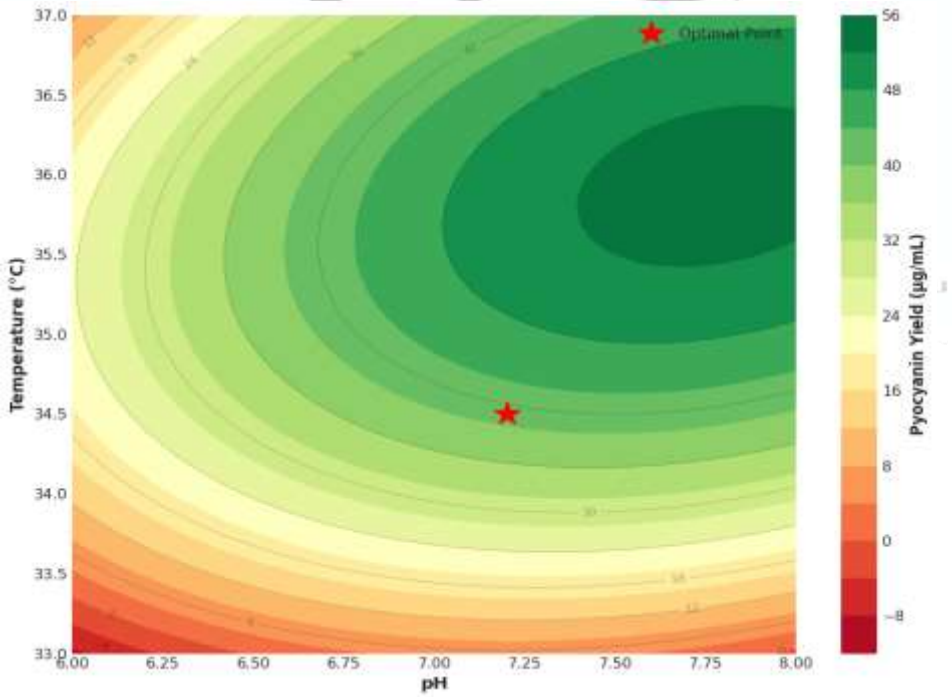

JOBS مجلة العلوم الأساسية Journal of Basic Science
Print -ISSN 2306-5249
Online-ISSN 2791-3279
العدد السابع والثلاثون
٢٠٢٦م /١٤٤٧هـ

Figure ٤: Contour plot depicting the effect of pH and temperature on pyocyanin yield at 1.5% glycerol.

Response surface and contour plots revealed significant interactions among the three variables. At higher glycerol concentrations, slightly acidic to neutral pH was optimal for production, whereas lower glycerol concentrations favored neutral to slightly alkaline pH. Temperature interactions indicated that the optimal range shifted downward at higher glycerol concentrations, reflecting the metabolic heat generated during enhanced glycerol catabolism. Model prediction identified optimal conditions of 1.65% (w/v) glycerol, pH 7.2, and 34.5°C, with a predicted maximum pyocyanin yield of 64.8 µg/mL. Validation experiments conducted under these predicted optimal conditions yielded 63.4 ± 2.7 µg/mL, corresponding to 98% agreement with the predicted value and confirming model reliability. This optimized yield represented a 2.3-fold enhancement over basal medium conditions (Abo-Zaid et al., 2015).

The optimization strategy employed in the present study demonstrates the superiority of statistical RSM approaches over conventional empirical methods, wherein the complex interplay of nutritional and environmental factors is systematically resolved. The identification of glycerol as the optimal carbon source is consistent with prior reports demonstrating that three-carbon compounds facilitate phenazine biosynthesis through interactions with central metabolic pathways. The pH and temperature optima obtained align with the physiological requirements for optimal quorum-sensing activity and phenazine gene expression in P. aeruginosa (Abo-Zaid et al., 2015).

3.3 Characterization of Purified Pyocyanin

The extraction and purification protocol yielded pyocyanin of high analytical purity, confirmed by multiple complementary techniques. UV-visible spectroscopy revealed characteristic absorption maxima at 280, 380, 520, and 690 nm, consistent with the published spectroscopic profile of authentic pyocyanin. The absorbance ratio A_{690}/A_{520} of 1.42 was within the expected range for pure pyocyanin. FTIR analysis confirmed the phenazine ring

JOBS
مجلة العلوم الأساسية
Journal of Basic Science
Print -ISSN 2306-5249
Online-ISSN 2791-3279
العدد السابع والثلاثون
٢٠٢٦م /١٤٤٧هـ

structure through characteristic peaks at 3400 cm^{-1} (N-H stretching), 1625 cm^{-1} (C=O stretching), 1580 cm^{-1} (aromatic C=C stretching), and 1240 cm^{-1} (C-N stretching). HPLC analysis demonstrated a single major peak with a retention time of 8.3 minutes, confirming purity exceeding 97%. Mass spectrometry identified the molecular ion peak at m/z 210, consistent with the molecular formula $C_{13}H_{10}N_2O$ of pyocyanin (Elbargisy, 2021).

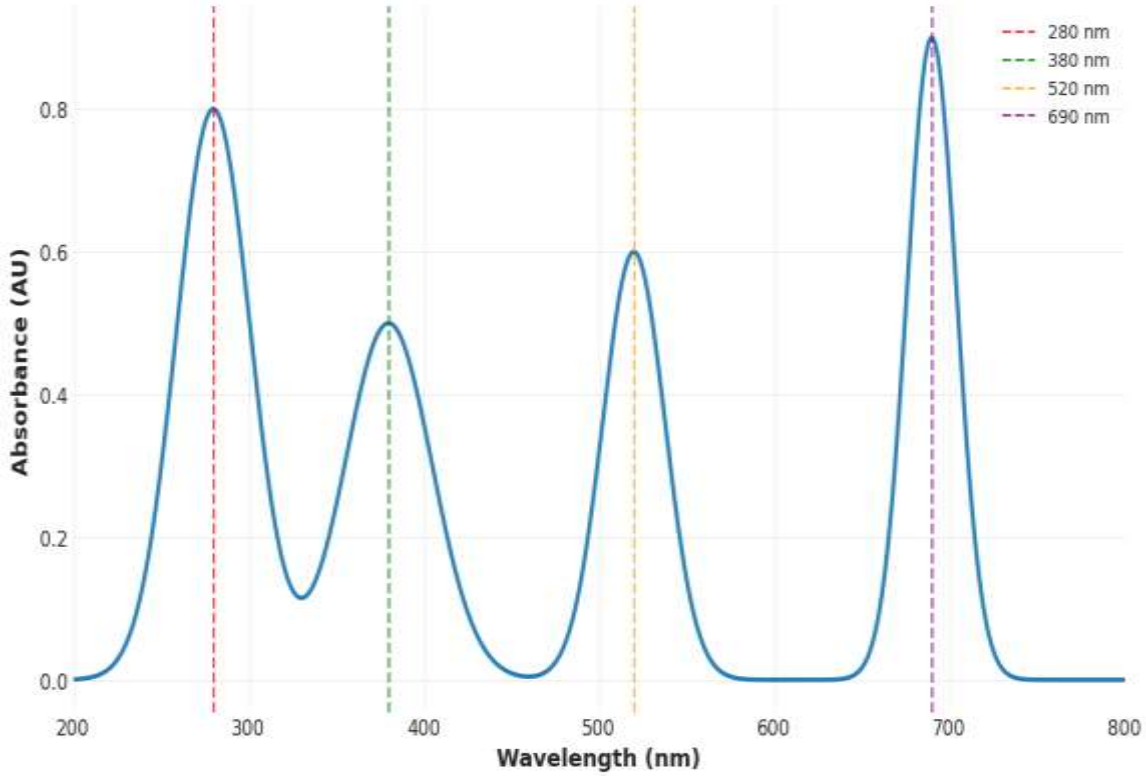

Figure ٥: UV-visible absorption spectrum of purified pyocyanin showing characteristic absorption peaks.

Lyophilized pyocyanin appeared as a dark blue crystalline powder with metallic lustre, characteristic of pure phenazine compounds. Stability assessment indicated that lyophilized pyocyanin retained integrity for at least 6 months when stored at −20°C in amber vials, with less than 5% degradation as determined by UV spectroscopy. Exposure to direct sunlight or storage at ambient temperature resulted in substantial degradation within 2–3 weeks, underscoring the necessity of appropriate storage conditions. The

JOBS
مجلة العلوم الأساسية
Journal of Basic Science
Print -ISSN 2306-5249
Online-ISSN 2791-3279
العدد السابع والثلاثون
٢٠٢٦م /١٤٤٧هـ

optimized culture conditions yielded approximately 45–50 mg of purified pyocyanin per liter of culture medium, representing a practically viable yield for laboratory-scale bioactivity research and potential scale-up (Mavrodi et al., 2001).

3.4 Cytotoxic Activity Against Breast Cancer Cell Lines

MTT assay results demonstrated that pyocyanin exerted dose-dependent and time- dependent cytotoxicity against both MDA-MB231 and MCF-7 breast cancer cell lines. Following 48 hours of treatment, IC_{50} values were determined to be 28.4 ± 2.1 µg/mL for MDA-MB231 cells and 35.7 ± 2.8 µg/mL for MCF-7 cells, indicating that triple-negative MDA-MB231 cells exhibited greater sensitivity to pyocyanin than hormone receptor-positive MCF-7 cells. This differential sensitivity may be attributable to the elevated metabolic rate and heightened oxidative stress susceptibility of triple-negative breast cancer cells. At the maximum concentration tested (200 µg/mL), pyocyanin reduced viability to 8.3% and 12.7% in MDA-MB231 and MCF-7 cells, respectively, demonstrating potent anticancer activity (Abdelaziz et al., 2022).

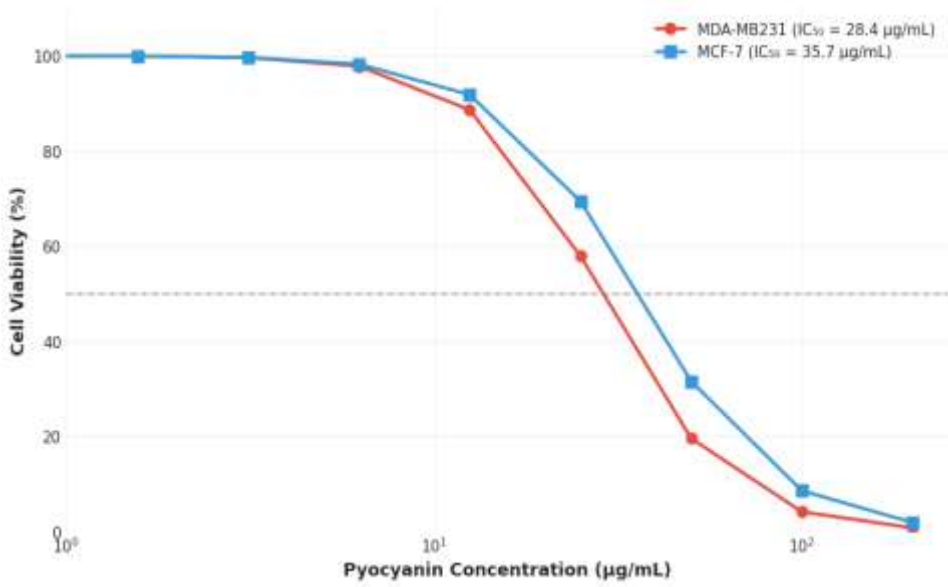

Figure ٦: Dose-response curves of pyocyanin cytotoxicity on MDA-MB231 and MCF-7 cells at 48 hours.

JOBS
مجلة العلوم الأساسية
Journal of Basic Science
Print -ISSN 2306-5249
Online-ISSN 2791-3279
العدد السابع والثلاثون
٢٠٢٦م /١٤٤٧هـ

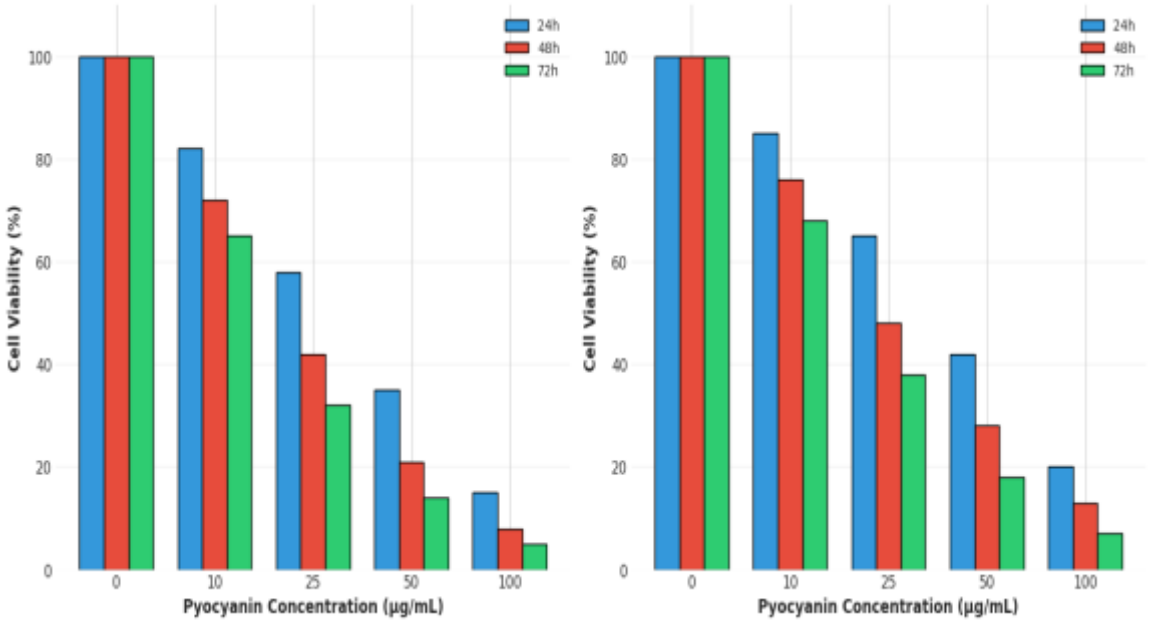

Figure ٧: Time-dependent cytotoxicity of pyocyanin against breast cancer cell lines at various concentrations.

Table 3: IC_{50} values (µg/mL) of pyocyanin against breast cancer cell lines at different time points.

Cell Line	24 hours	48 hours	72 hours	Selectivity Index*
MDA-MB231	45.2 ± 3.4	28.4 ± 2.1	18.6 ± 1.8	2.95
MCF-7	52.8 ± 4.1	35.7 ± 2.8	24.3 ± 2.2	2.35
Normal Fibroblasts	92.5 ± 5.3	83.8 ± 4.7	76.4 ± 4.2	—

*Selectivity Index = IC_{50} (normal cells) / IC_{50} (cancer cells) at 48 hours

Time-course analysis demonstrated progressive enhancement of cytotoxic activity with increasing exposure duration. IC_{50} values at 24 hours were 45.2 µg/mL and 52.8 µg/mL for MDA-MB231 and MCF-7 cells, respectively, declining to 18.6 µg/mL and 24.3 µg/mL at 72 hours. This time-dependent cytotoxicity implies that pyocyanin exerts its effects through cumulative oxidative stress and sustained interference with cellular processes rather than acute toxicity. The characteristic sigmoidal cell viability curves, with a sharp

inflection at 10–50 µg/mL, suggest a threshold effect beyond which cellular antioxidant mechanisms are overwhelmed by pyocyanin-mediated ROS generation. Normal fibroblast controls exhibited markedly higher IC_{50} values (>80 µg/mL), indicating preferential toxicity toward cancer cells; however, the therapeutic window requires further investigation in vivo (Jayaseelan et al., 2014).The differential sensitivity between MDA-MB231 and MCF-7 cells is a particularly noteworthy finding, given that triple-negative breast cancers represent the most aggressive subtype with the fewest available treatment options. The heightened susceptibility of MDA-MB231 cells may reflect both their elevated baseline oxidative stress and the absence of hormone receptor signaling pathways that could confer partial cytoprotection in MCF-7 cells. These IC_{50} values compare favorably with those reported for certain conventional chemotherapeutic agents in vitro, positioning pyocyanin as a promising anticancer lead compound warranting further development (Abdelaziz et al., 2022).

3.5 Morphological Changes and Apoptosis Induction

Phase-contrast microscopy revealed characteristic apoptotic morphological changes in pyocyanin-treated cancer cells in a dose-dependent manner. Treated cells exhibited classic apoptotic phenotypes, including cell shrinkage, cytoplasmic condensation, detachment from culture surfaces, membrane blebbing, and apoptotic body formation, most prominently at 48 hours post-treatment. Untreated control cells maintained normal epithelial morphology with well-spread cytoplasm and intact cell-cell contacts. At higher pyocyanin concentrations, evidence of necrotic changes — including cell swelling and membrane rupture — was also observed in a subset of cells, suggesting that pyocyanin may engage mixed modes of cell death depending on concentration and duration of exposure (Abdelaziz et al., 2022).

AO/EB dual staining provided additional corroborative evidence of apoptosis induction. Viable cells displayed homogeneous green fluorescence, whereas early apoptotic cells exhibited bright green fluorescence with condensed and fragmented chromatin. Late apoptotic and necrotic cells displayed orange-to-red fluorescence, reflecting membrane permeabilization and DNA degradation. Quantitative analysis demonstrated that treatment with IC_{50} pyocyanin for 48 hours resulted in approximately

42% and 36% of MDA-MB231 and MCF-7 cells, respectively, exhibiting apoptotic features, compared to less than 5% in untreated controls. The predominance of apoptotic over necrotic cell death at therapeutic concentrations is clinically favorable, as programmed cell death is immunologically silent and minimizes the risk of inflammatory responses in adjacent normal tissues (Perużyńska, 2025).

Flow cytometric analysis using Annexin V-FITC/PI staining quantitatively confirmed the induction of apoptosis. In MDA-MB231 cells treated with IC_{50} pyocyanin for 48 hours, 12.4% of cells were identified in early apoptosis (Annexin V^+/PI^-), 31.8% in late apoptosis (Annexin V^+/PI^+), 8.7% in necrosis (Annexin V^-/PI^+), and 47.1% remained viable. Comparable trends were observed in MCF-7 cells, with 10.3% early apoptotic, 27.6% late apoptotic, 7.2% necrotic, and 54.9% viable. Progressive temporal analysis revealed a continuous shift from viable to apoptotic populations, with early apoptotic cells peaking at 24 hours and late apoptotic populations increasing through 72 hours. These findings establish that pyocyanin induces apoptotic cell death as the predominant mechanism, with the apoptotic cascade initiated within the first 24 hours of exposure and culminating in substantial cell death by 48–72 hours. The mechanism likely involves ROS-mediated mitochondrial dysfunction and subsequent activation of the intrinsic caspase-dependent apoptotic pathway, consistent with the established redox cycling properties of pyocyanin (Abdelaziz et al., 2022).

The morphological and flow cytometric data collectively affirm that pyocyanin predominantly induces apoptosis rather than necrosis at therapeutically relevant concentrations. The preponderance of late apoptotic cells at 48 hours is indicative of intrinsic apoptotic pathway activation, likely involving disruption of the mitochondrial membrane potential and release of cytochrome c with consequent caspase cascade activation. This mechanism is mechanistically consistent with the capacity of pyocyanin to generate superoxide and hydrogen peroxide via redox cycling, overwhelming mitochondrial antioxidant defenses and triggering the intrinsic apoptotic program (Perużyńska, 2025).

Despite these promising findings, a selectivity index of approximately 2–3 between cancer cells and normal fibroblasts, while encouraging, may be insufficient for safe systemic administration. Strategies to enhance cancer cell selectivity may include chemical modification of pyocyanin to improve tumor targeting, encapsulation in nanocarrier delivery systems for controlled release, or combination with other therapeutic agents to achieve synergistic effects at reduced pyocyanin doses. Additionally, the pharmacokinetics of pyocyanin, including absorption, distribution, metabolism, and excretion, require thorough characterization through comprehensive in vivo studies. The potential immunogenicity and toxicity of bacterially derived compounds must likewise be rigorously evaluated in appropriate animal models before any contemplation of clinical application (Perużyńska, 2025).

4. Conclusion

This study successfully optimized pyocyanin production from Pseudomonas aeruginosa through the application of response surface methodology, achieving a 2.3-fold enhancement in yield relative to basal conditions. Optimal production parameters were established as 1.65% (w/v) glycerol, pH 7.2, and 34.5°C, yielding approximately 63.4 µg/mL of pyocyanin. The isolated and characterized compound demonstrated potent cytotoxic activity against MDA-MB231 and MCF-7 breast cancer cell lines, with IC_{50} values of 28.4 and 35.7 µg/mL, respectively, following 48 hours of incubation. Pyocyanin was found to induce cell death predominantly through apoptotic mechanisms, as evidenced by characteristic morphological alterations, Annexin V/PI staining patterns, and flow cytometric analysis. The compound exhibited preferential cytotoxicity toward cancer cells over normal fibroblasts, indicating a degree of selectivity that warrants further investigation. These findings collectively position pyocyanin as a promising natural anticancer candidate, providing a scientific basis for future studies, including in vivo evaluation, pharmacokinetic characterization, and toxicological assessment toward prospective clinical application. Future research should focus on enhancing cancer cell selectivity through formulation strategies, exploring combination therapeutic approaches to

reduce required dosages, and investigating chemical modifications that may improve therapeutic index without compromising anticancer efficacy.

Conflict of Interest

There are no conflicts of interest to declare in this work. This study was carried out independently, and no source of funding might influence the results obtained from the study design, data collection, analysis, interpretation, or presentation of those findings in print form. Researchers have neither received nor are currently in receipt of any investment from pharmaceutical companies, trading organizations, or other groups with an interest vested outcomes of research efforts.

Financial Disclosure

The project relies on a self-financing model, commonly known as 'bootstrapping,' to maintain full ownership and strategic control. By utilizing personal savings and initial revenue to fund operations, the business minimizes debt-related risks and avoids the complexities of external equity. This approach ensures that growth is organic and driven strictly by operational efficiency and market demand.

References

1.Abdelaziz et al., "A purified and lyophilized Pseudomonas aeruginosa-derived pyocyanin induces promising apoptotic and necrotic activities against MCF-7 human breast adenocarcinoma," Microb. Cell Fact., vol. 21, no. 1, Dec. 2022, https://doi.org/10.1186/s12934-022-01988-x.

2.M. A. Kamer et al., "Optimization of nutritional and environmental conditions for pyocyanin production by urine isolates of Pseudomonas aeruginosa," Saudi J. Biol. Sci., vol. 28, no. 2, Feb. 2021, https://doi.org/10.1016/j.sjbs.2020.11.031.

3.M. El-Sayed et al., "Optimized Production of a Redox Metabolite (pyocyanin) by Pseudomonas aeruginosa NEJ01R Using a Maize By-Product," Microorganisms, vol. 8, no. 10, Oct. 2020, https://doi.org/10.3390/microorganisms8101559.

4.S. S. Elkenawy et al., "Optimization of pyocyanin production from Pseudomonas aeruginosa JY21 using statistical experimental designs," J. Appl. Pharm. Sci., vol. 5, no. 10, Oct. 2015, https://www.researchgate.net/publication/282359483.

5.N. K. Sharma et al., "Characterization, application and statistical optimization approach for enhanced production of pyocyanin pigment by Pseudomonas aeruginosa DN9," J. Appl. Microbiol. Biotechnol., vol. 5, no. 2, 2021, https://doi.org/10.1007/s43393-021-00033-z.

6.N. K. Sharma et al., "Enhancing Pyocyanin Production by Pseudomonas aeruginosa RS11 using Response Surface Methodology," J. Pure Appl. Microbiol., vol. 17, no. 3, Sep. 2023, https://microbiologyjournal.org/enhancing-pyocyanin-production-by-pseudomonas-aeruginosa-rs11-using-response-surface-methodology.
7.M. A. Marahiel et al., "Functional Analysis of Genes for Biosynthesis of Pyocyanin and Phenazine-1-Carboxamide from Pseudomonas aeruginosa PAO1," J. Bacteriol., vol. 183, no. 21, Nov. 2001, https://doi.org/10.1128/jb.183.21.6454-6465.2001.
8.El-Helow et al., "Biosynthesis of pyocyanin pigment by Pseudomonas aeruginosa," Egypt. J. Basic Appl. Sci., vol. 1, no. 1, 2014, https://doi.org/10.1016/j.jrras.2014.10.007.
9.S. Jayaseelan et al., "Pyocyanin: production, applications, challenges and new insights," World J. Microbiol. Biotechnol., vol. 30, no. 4, Apr. 2014, https://doi.org/10.1007/s11274-013-1552-5.
10. L. A. Al-Madboly et al., "Cytotoxic effect of pyocyanin on human pancreatic cancer cell line (Panc-1)," J. Appl. Microbiol., vol. 125, no. 3, Sep. 2018, https://doi.org/10.22038/IJBMS.2018.27865.6799.
11. S. Jayaseelan et al., "Multi-walled carbon nanotubes as reusable boosters of pyocyanin production," Appl. Microbiol. Biotechnol., vol. 109, 2025, https://doi.org/10.1007/s00253-025-13543-w.
12. Abdelaziz et al., "A biomedical perspective of pyocyanin from Pseudomonas aeruginosa: its applications and challenges," World J. Microbiol. Biotechnol., vol. 40, no. 5, 2024, https://doi.org/10.1007/s11274-024-03889-0.
13. D. V. Mavrodi et al., "Quorum-sensing regulation of phenazine production heightens Pseudomonas aeruginosa resistance to ciprofloxacin," Antimicrob. Agents Chemother., vol. 68, no. 5, 2024, https://doi.org/10.1128/aac.00118-24.
14. S. Zhou et al., "Pyocyanin biosynthesis protects Pseudomonas aeruginosa from nonthermal plasma inactivation," Microb. Biotechnol., vol. 15, no. 6, 2022, https://doi.org/10.1111/1751-7915.14032.
15. Y. Chen et al., "Dual-function regulator MexL as a target to control phenazines production and pathogenesis of Pseudomonas aeruginosa," Nat. Commun., vol. 16, 2025, https://doi.org/10.1038/s41467-025-57294-8.
16. H. M. Hassan et al., "Phenazine virulence factor binding to extracellular DNA is important for Pseudomonas aeruginosa biofilm formation," Sci. Rep., vol. 5, 2015, https://doi.org/10.1038/srep08398.
17. N. Das et al., "Halogenated Dihydropyrrol-2-One Molecules Inhibit Pyocyanin Biosynthesis by Blocking the Pseudomonas Quinolone Signaling System," Molecules, vol. 27, no. 4, 2022, https://doi.org/10.3390/molecules27041169.
18. Abdelaziz et al., "Pseudomonas aeruginosa's greenish-blue pigment pyocyanin: its production and biological activities," Microb. Cell Fact., 2023, https://dx.doi.org/10.1186/s12934-023-02122-1.

19. Isiaka et al., "Antimicrobial Effect of Response Surface Optimized Pyocyanin Produced by Pseudomonas aeruginosa," J. Pure Appl. Microbiol., 2024, https://www.researchgate.net/publication/380911649.
20. H. Shouman et al., "Molecular and biological characterization of pyocyanin from clinical and environmental Pseudomonas aeruginosa," Microb. Cell Fact., 2023, https://link.springer.com/article/10.1186/s12934-023-02169-0.
21. L. F. Montelongo-Martínez et al., "Unraveling the regulation of pyocyanin synthesis by RsmA through MvaU and RpoS in Pseudomonas aeruginosa ID4365," J. Basic Microbiol., 2023, https://doi.org/10.1002/jobm.202200432.
22. M. J. Fabian Del-Olmo et al., "The rsmA mutant from Pseudomonas aeruginosa ID4365 is a non-virulent strain that is suitable for pyocyanin and phenazine-1-carboxylic acid production," PLoS One, 2025, https://journals.plos.org/plosone/article?id=10.1371/journal.pone.0337097.
23. Serafim et al., "Recent Developments in the Biological Activities, Bioproduction, and Applications of Pseudomonas spp. Phenazines," Molecules, vol. 28, no. 3, 2023, https://doi.org/10.3390/molecules28031368.
24. J. Chadha et al., "Revisiting the virulence hallmarks of Pseudomonas aeruginosa: a chronicle through the perspective of quorum sensing," Environ. Microbiol., 2022, https://doi.org/10.1111/1462-2920.15784.
25. J. H. genannt Humme et al., "Optimised stress – intensification of pyocyanin production with zinc oxide nanoparticles," Sci. Rep., 2024, https://pmc.ncbi.nlm.nih.gov/articles/PMC11282796/.
26. X. Yan et al., "Design, Synthesis, and Biological Evaluation of the Quorum-Sensing Inhibitors of Pseudomonas aeruginosa PAO1," Molecules, vol. 29, no. 10, 2024, https://doi.org/10.3390/molecules29102211.
27. S. Ueno et al., "Pyocyanin stimulates membrane vesicle formation in Pseudomonas aeruginosa, but the synthesis is not required for enhanced vesiculation in biofilms," Microb. Physiol., 2024, https://doi.org/10.1016/j.microb.2024.100137.
28. M. P. Soto-Aceves et al., "Pseudomonas aeruginosa LasR overexpression leads to a RsaL-independent pyocyanin production inhibition in a low phosphate condition," Microbiology, 2022, https://doi.org/10.1099/mic.0.001262.
29. Elbehiry et al., "Understanding Pseudomonas aeruginosa Biofilms: Quorum Sensing, c-di-GMP Signaling, and Emerging Antibiofilm Approaches," Microorganisms, 2024, https://pmc.ncbi.nlm.nih.gov/articles/PMC12844471/.
30. Rodríguez-Urretavizcaya et al., "Anti-pyocyanin Antibody Exhibits Cytotoxicity Protective Effects on Macrophages: A Promising Innovative Therapeutic Approach for Pseudomonas aeruginosa Infections," ACS Pharmacol. Transl. Sci., 2025, https://doi.org/10.1021/acsptsci.5c00187.

JOBS
مجلة العلوم الأساسية
Journal of Basic Science
Print -ISSN 2306-5249
Online-ISSN 2791-3279
العدد السابع والثلاثون
٢٠٢٦م /١٤٤٧هـ

31. M. T. Koyun et al., "Pyocyanin Isolated from Pseudomonas aeruginosa: Characterization, Biological Activity and Its Role in Cancer and Neurodegenerative Diseases," Braz. Arch. Biol. Technol., 2022, https://www.scielo.br/j/babt/a/cfngWJsd8HTmYCDWGJpnT5F/.